

Effective synthesis of cis-3-hexen-1-yl acetate via transesterification over KOH/ γ -Al₂O₃: Structure and catalytic performance

Xiaoshuan Li^a, Dinghua Yu^{b,c}, Wengui Zhang^b, Zhengwen Li^b, Xiaowei Zhang^b, He Huang^{b,c,*}

^a School of Pharmaceutical Sciences, Nanjing University of Technology, Nanjing 210009, China

^b College of Biotechnology and Pharmaceutical Engineering, Nanjing University of Technology, Nanjing 210009, China

^c State Key Laboratory of Materials-Oriented Chemical Engineering, Nanjing University of Technology, Nanjing 210009, China

ARTICLE INFO

Article history:

Received 5 August 2012

Received in revised form 11 January 2013

Accepted 12 January 2013

Available online xxx

Keywords:

Cis-3-hexen-1-yl acetate

Cis-3-hexen-1-ol

Transesterification

KOH/ γ -Al₂O₃

Flavor

ABSTRACT

Cis-3-hexen-1-yl acetate is a significant green note flavor compound and widely used in the food and cosmetic industry. In this research, a series of solid base KOH/ γ -Al₂O₃ have been prepared and been utilized for the synthesis of cis-3-hexen-1-yl acetate via transesterification from cis-3-hexen-1-yl and ethyl acetate. The catalysts were also characterized by several physic-chemical techniques such as X-ray diffraction (XRD), Fourier transform infrared (FT-IR) spectroscopy, N₂ adsorption, CO₂-temperature-programmed desorption (CO₂-TPD), and X-ray fluorescence (XRF). 30%KOH/Al₂O₃ was suggested to be the best conversion due to the cis-3-hexen-1-ol conversion of 59.3% at a temperature 88 °C within 2 h. Characterization results showed that KOH transformed into Al–O–K and K₂O–CO₂ species during the calcination process. It was confirmed that K₂O–CO₂ disappeared and Al–O–K groups existed on the surface of the water-washing 30%KOH/Al₂O₃ which was inactive for transesterification. K₂O–CO₂ species might be the major active species on KOH/Al₂O₃, and Al–O–K groups was inactive for cis-3-hexen-yl acetate synthesis.

© 2013 Elsevier B.V. All rights reserved.

1. Introduction

Hexyl esters (i.e. cis-3-hexen-1-yl acetate) are extremely aromatic compound with ‘green notes’ flavor and widely used in the food and cosmetic industry [1,2]. The present demands for natural flavors are estimated to be 5–10 metric tons annually at price of 2500–6000 US/kg, while the demands are not fulfilled by the current production capacity [3]. Traditionally, they have been isolated from high plants [3]. Nowadays, cis-3-hexen-1-yl acetate, caproate and butyrate have been mostly synthesized via esterification process over enzymes [3–8]. However, enzyme catalysts remain an important consideration to the manufacturers for their high cost and long reaction period (>24 h). In addition, some catalysts such as metallic chlorides [9] and perchlorates [10] have been also developed for the synthesis of cis-hexen-1-yl esters via esterification, while the removal of residual metallic salts in products becomes a problem. Therefore, the synthesis of such esters needs to reduce the product cost in most favorable conditions.

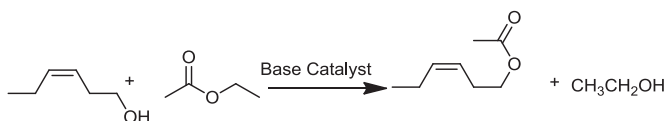
Theoretically, cis-3-hexen-1-yl acetate also can be synthesized via transesterification catalyzed by solid base. Solid base is always

considered as a kind of effective and green catalyst, which minimizes the difficulty in separation and recovery processes usually encountered with conventional base. From reported articles, solid base has been tried extensively for biodiesel [11–13], diethyl carbonate [14,15], methyl propyl carbonate [16,17], polycarbonate diols [18], and other fine chemicals. Among the solid base catalysts, modified γ -Al₂O₃ has been widely used in a number of base-catalyzed reactions as a heterogeneous base catalyst [19–21], especially, transesterification [21–25]. K. Noiroj and W. Xie et al. did excellent work in biodiesel production over γ -Al₂O₃ modified by potassium salt [22,26–28], and found that high activity for transesterification could be attributed to the strongly basic nature of catalysts. However, there are few reports on this alternative synthesis of cis-3-hexen-1-yl acetate over solid base catalyst from cis-3-hexen-1-ol and ethyl acetate catalyzed by a solid base (Scheme 1).

In this research, solid base catalysts were prepared from a commercial γ -Al₂O₃ modified by KOH solutions and firstly used for the production of cis-3-hexen-1-yl acetate (see Scheme 1). KOH/Al₂O₃ was prepared by impregnation and applied to determine the optimum conditions for cis-3-hexen-1-yl acetate. Several factors which may influence the quality of cis-3-hexen-1-yl acetate were investigated, including wt% of KOH loading on Al₂O₃, amount of catalyst, molar ratio cis-3-hexen-1-ol to ethyl acetate, reaction time and temperature. Moreover, the stability of the catalyst and

* Corresponding author at: Nanjing University of Technology, No.5 Ximofan Road, Nanjing 210009, China. Tel.: +86 25 83172094; fax: +86 25 83172094.

E-mail address: biotech@njut.edu.cn (H. Huang).



Scheme 1. Synthesis of cis-3-hexen-1-yl acetate via transesterification.

water-washing catalyst was also discussed. Furthermore, the active sites of $\text{KOH}/\text{Al}_2\text{O}_3$ catalysts were discussed, and a plausible reaction mechanism for transesterification was proposed.

2. Experimental

2.1. Catalyst preparation

$\text{KOH}/\gamma\text{-Al}_2\text{O}_3$ catalysts were prepared by wet impregnation method. Powder $\gamma\text{-Al}_2\text{O}_3$ was calcined in a muffle furnace at 500°C for 3 h before catalyst preparation. Typically, 20 g $\gamma\text{-Al}_2\text{O}_3$ was impregnated into 50 ml KOH solution at 40°C for 3 h, and water was removed under 90°C . The precursor was dried at 120°C overnight and stored in a vacuum desiccator. Prior to the reaction, the precursor was activated in a muffle furnace at 500°C for 3 h. For convenience, the catalysts were designated as 10% $\text{KOH}/\text{Al}_2\text{O}_3$, 20% $\text{KOH}/\text{Al}_2\text{O}_3$, 30% $\text{KOH}/\text{Al}_2\text{O}_3$, 40% $\text{KOH}/\text{Al}_2\text{O}_3$. 30% $\text{KOH}/\text{Al}_2\text{O}_3$ was mean for 30 wt.% of KOH with respect to $\gamma\text{-Al}_2\text{O}_3$ and KOH.

Reusability tests were conducted over 30% $\text{KOH}/\text{Al}_2\text{O}_3$. The first method was that the used 30% $\text{KOH}/\text{Al}_2\text{O}_3$ was filtered, dried at 120°C overnight after each test. The second method was that the used 30% $\text{KOH}/\text{Al}_2\text{O}_3$ was filtered, dried at 120°C overnight, and calcined at 500°C for 3 h after each test. During the second method procedure, after the first reused catalyst calcined at 500°C for 3 h was called 30% $\text{KOH}/\text{Al}_2\text{O}_3\text{-U1}$, after the second reused one was 30% $\text{KOH}/\text{Al}_2\text{O}_3\text{-U2}$, after the third was 30% $\text{KOH}/\text{Al}_2\text{O}_3\text{-U3}$, and after the fourth was 30% $\text{KOH}/\text{Al}_2\text{O}_3\text{-U4}$. 30% $\text{KOH}/\text{Al}_2\text{O}_3$ was washed by water, until the water going through the catalyst was neutral. The washed catalyst was named 30% $\text{KOH}/\text{Al}_2\text{O}_3\text{-W}$, which was then dried at 120°C overnight, and calcined at 500°C for 3 h.

2.2. Catalyst characterization

The XRD measurements were performed on a Philips X'Pro X-ray diffractometer with a $\text{Cu K}\alpha$ irradiation, over a 2θ range of $10\text{--}90^\circ$ with a step size of 0.02° . The X-ray source was operated at 40 kV and 40 mA. The phases were identified using the Powder Diffraction File (PDF) database (JCPDS, International Centre for Diffraction Date).

FT-IR spectra were recorded on a Nicolet 670 spectrometer during $4000\text{--}400\text{ cm}^{-1}$, with 2 cm^{-1} resolution. The KBr pellet technique was applied for preparing samples. All measurements were conducted at room temperature.

N_2 adsorption/desorption isotherms were measured at -196°C , using a Micromeritics ASAP 2020 analyzer. The sample was pre-treated at 250°C in a vacuum for 48 h before measurements. Surface areas were calculated using the Brunauer–Emmett–Teller (BET) model. Pore volumes were estimated from desorption branches of nitrogen isotherms using the Barret–Joyner–Halenda (BJH) model.

Temperature-programmed desorption (TPD) of carbon dioxide was performed in a BEL-CAT-B-82 equipment. The sample was first calcined at 500°C for 3 h and subsequently cooled to 100°C under a helium flow (30 mL/min), saturated with dry gaseous carbon dioxide (99.999%, 50 mL/min) at 100°C for 30 min. The sample was then purged with a helium flow (30 mL/min) for 30 min. The CO_2 -TPD performed at a rate of $10^\circ\text{C}/\text{min}$ to 750°C , and kept for 90 min at 750°C .

Energy dispersive X-ray fluorescence (XRF) spectrometry was performed using a Switzerland ARL9800 XRF.

2.3. Catalytic activity measurements

The transesterification of cis-3-hexen-1-ol (Nippon Zeon Co., Ltd) with ethyl acetate (Sinopharm Chemical Reagent Co., Ltd) was carried out in a 100 mL jacketed two-necked glass round bottom flask, equipped with a long spiral condenser connected to water circulation and a temperature-controlled magnetic stirrer. The desired amount of cis-3-hexen-1-ol, ethyl acetate and catalyst was added into the flask. The reaction was carried out until it reached the desired reaction time. After that, the reaction was stopped by cooling the reactor to room temperature and the catalyst was separated from the liquid phase by filtration. All experiments were performed under atmospheric pressure.

2.4. Product analysis

Analysis of the reaction products were conducted by an Agilent 6890N gas chromatograph equipped with a flame ionization detector and a HP-FFAP column (30 m \times 0.53 mm, film thickness $1\ \mu\text{m}$). The carrier gas was N_2 (2 mL/min, split). The GC oven temperature was maintained at 60°C for 2 min and then increased to 210°C at a rate of $10^\circ\text{C}/\text{min}$ and held for 4 min. The injector temperature was fixed 250°C and the detector temperature was at 240°C . The GC was connected to a chemstation which recorded the peak areas and retention times in the chromatogram. Cis-3-hexen-yl acetate was identified by the retention times. The cis-3-hexen-1-ol conversion and the cis-3-hexen-1-yl acetate selectivity were calculated using:

Conversion_{cis-3-hexen-1-ol} (%)

$$= \frac{M_{\text{initial cis-3-hexen-1-ol}} - M_{\text{final cis-3-hexen-1-ol}}}{M_{\text{initial cis-3-hexen-1-ol}}} \times 100$$

Selectivity_{cis-hexen-1-yl acetate} (%)

$$= \frac{M_{\text{cis-hexen-yl acetate}}}{M_{\text{initial cis-3-hexen-1-ol}} - M_{\text{final cis-3-hexen-1-ol}}} \times 100$$

where $M_{\text{initial cis-3-hexen-1-ol}}$ refers to additional cis-hexen-1-ol, $M_{\text{final cis-3-hexen-1-ol}}$ refers to the cis-hexen-1-ol in the product after reaction, and $M_{\text{cis-hexen-1-yl acetate}}$ refers to the cis-hexen-1-yl from cis-hexen-1-ol in the product after reaction. They were determined by quantitative analysis using relative molar calibration factor.

3. Results and discussion

3.1. Catalyst characterization

3.1.1. X-ray diffraction

The XRD patterns of $\gamma\text{-Al}_2\text{O}_3$, and $\text{KOH}/\text{Al}_2\text{O}_3$ were performed to determine the change of crystal structure in the catalysts, and the corresponding results were shown in Fig. 1. Fresh $\gamma\text{-Al}_2\text{O}_3$ exhibited the typical diffraction peaks of $\gamma\text{-Al}_2\text{O}_3$ at 2θ value of 37° , 46° , and 67° . With the increasing amount of loaded KOH from 10% to 40%, the intensities of the typical diffraction peaks (37° , 46° , and 67°) decreased, demonstrating the strong interaction between KOH and $\gamma\text{-Al}_2\text{O}_3$ [27,28]. As the amount loading of KOH exceeded 20%, the diffraction peak at 2θ value of 37° almost disappeared and new diffraction peaks at 2θ value of 20° , 29° , 33° , 34° , 39° , 41° , 47° , 59° and 69° (JCPDS 01-089-8451) appeared, which were ascribed to orthorhombic $\alpha\text{-KAlO}_2$ species formed on the catalyst surface [29]. When the KOH amount was up to 40%, the new phase of $\alpha\text{-KAlO}_2$ was obviously observed in Fig. 1. It could be deduced that KOH reacted with $\gamma\text{-Al}_2\text{O}_3$ generating new phase of Al–O–K groups

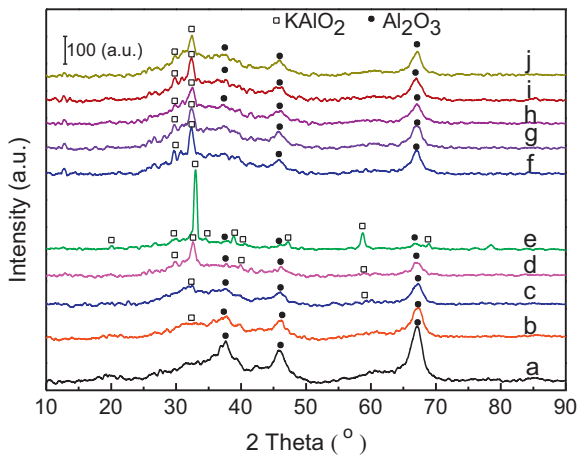


Fig. 1. XRD patterns. (a) γ - Al_2O_3 ; (b) 10%KOH/ Al_2O_3 ; (c) 20%KOH/ Al_2O_3 ; (d) 30%KOH/ Al_2O_3 ; (e) 40%KOH/ Al_2O_3 ; (f) 30%KOH/ Al_2O_3 -U1; (g) 30%KOH/ Al_2O_3 -U2; (h) 30%KOH/ Al_2O_3 -U3; (i) 30%KOH/ Al_2O_3 -U4; (j) 30%KOH/ Al_2O_3 -W.

in the composite [21,27] during the calcination at 500 °C for 3 h, which agreed with low-temperature form of α - KAlO_2 [29].

The patterns of the used 30%KOH/ Al_2O_3 and water-washing 30%KOH/ Al_2O_3 were shown in Fig. 1. The result showed that XRD patterns of all the repeated used catalysts had the same XRD patterns as that of the fresh 30%KOH/ Al_2O_3 and the intensities of the XRD patterns kept well after reusing four times. In other words, the new phase of Al–O–K groups still remained. The XRD patterns of the water-washing catalyst agreed well with the fresh 30%KOH/ Al_2O_3 . It was suggested that the new phase of Al–O–K compound could not react with water and not be destroyed by water.

3.1.2. FT-IR spectroscopy

FT-IR spectroscopy was used to investigate the functional groups in the catalysts. The results were shown in Fig. 2. There were two bands in curve at 3440 cm^{-1} and 1640 cm^{-1} attributed to the present of physical adsorbed water [22,30,31]. The two shoulders were assigned to the O–H stretching (3440 cm^{-1}) and the O–H bending (1640 cm^{-1}) of physical adsorbed water respectively. The water might come from the reaction of the promoter salt (KOH) with the γ - Al_2O_3 or the atmospheric H_2O during the calcination of the catalyst preparation. By the way, the band at 3440 cm^{-1} could be partly attributed to the stretching vibrations of Al–O–K

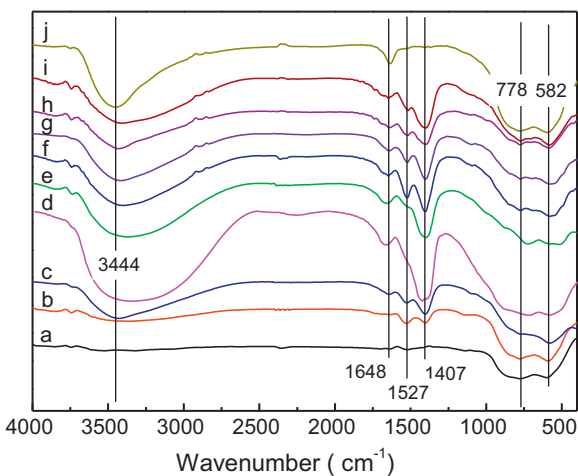


Fig. 2. FT-IR spectra. (a) γ - Al_2O_3 ; (b) 10% KOH/ Al_2O_3 ; (c) 20%KOH/ Al_2O_3 ; (d) 30%KOH/ Al_2O_3 ; (e) 40%KOH/ Al_2O_3 ; (f) 30%KOH/ Al_2O_3 -U1; (g) 30%KOH/ Al_2O_3 -U2; (h) 30%KOH/ Al_2O_3 -U3; (i) 30%KOH/ Al_2O_3 -U4; (j) 30%KOH/ Al_2O_3 -W.

groups [22,32–34]. From the spectra of KOH/ Al_2O_3 , there were two peaks at 1527 cm^{-1} and 1400 cm^{-1} . The intensity of the band at 1400 cm^{-1} increased with increasing amount of KOH on the catalyst, while its intensity at 1527 cm^{-1} decreased. The bands at 1527 cm^{-1} and 1400 cm^{-1} were due to CO_3^{2-} ions (chemisorbed CO_2) weakly bounded with K^+ present on the surface of the catalyst [30,35]. The CO_3^{2-} might be attributed to the chemical adsorbed CO_2 forming $\text{K}_2\text{O}\cdot\text{CO}_2$ species like K_2CO_3 during the calcination of the catalyst preparation. Therefore, $\text{K}_2\text{O}\cdot\text{CO}_2$ species were responsible for the peaks of K_2O not observed in the XRD patterns (see Fig. 1). The bands at 778 cm^{-1} (AlO_4 groups) and 582 cm^{-1} (AlO_6 groups) indicated the presence of Al–O–Al framework [32,36]. While the shoulders at 778 cm^{-1} decreased and shifted to a lower wavelength due to the effect of K^+ on the Al–O bonds (the Al–O bands were on AlO_4 groups). As shown in Fig. 2, the spectra of used 30%KOH/ Al_2O_3 showed the same spectra with that of fresh 30%KOH/ Al_2O_3 . However, there were not the bands at 1527 cm^{-1} and 1400 cm^{-1} on the spectra of the water-washing 30%KOH/ Al_2O_3 . The fact showed CO_3^{2-} has been washed by water.

3.1.3. BET surface area measurement

The BET surface area, average pore size and pore volume of the supports and catalysts were presented in Table 1. It was found that the BET surface area and the pore volume of the catalysts varied in a wide range 284.17 m^2/g to 50.59 m^2/g , and 0.53 cm^3/g to 0.11 cm^3/g , respectively. As listed in Table 1, the BET surface area and the pore volume of the catalysts decreased sharply with increasing amount of KOH. This might be due to that some smaller pores were blocked [27,32]. Meanwhile, the average pore sizes increased firstly with KOH amount below 20% and then decreased. The average pore size over the catalysts used for four times became large from 7.76 Å to 9.10 Å. This suggested some potassium species leached away. After washed by water, the catalyst showed different textural characteristics from that of Al_2O_3 . Combining with the results of XRD pattern and the FT-IR, it can be concluded that the species $\text{K}_2\text{O}\cdot\text{CO}_2$ was washed away, while KAlO_2 still existed on the surface.

3.1.4. CO_2 -TPD

The TPD profiles of desorbed CO_2 on γ - Al_2O_3 , KOH/ Al_2O_3 , used 30% KOH/ Al_2O_3 and water-washing 30%KOH/ Al_2O_3 were shown in Fig. 3, and the quantitative results were listed in Table 2. Fig. 3 showed there were mainly two desorption ranges at γ - Al_2O_3 , KOH/ Al_2O_3 , used 30% KOH/ Al_2O_3 curves. One was centered at around 150 °C and was assigned to the weak basic sites, and the second one was assigned to the strong basic sites at around 550 °C [37,38]. The basic strength increased after 30%KOH/ Al_2O_3 used, which was related to pore sizes (see Table 1). The water-washing 30%KOH/ Al_2O_3 catalyst had three peaks at 100 °C, 255 °C, and 550 °C, which meant the water-washing 30%KOH/ Al_2O_3 exited weak, intermediate, and strong basic sites [37,38]. As listed in Table 2, the total base amount of the catalysts changed significantly in the range of our research. The total base amount of KOH/ Al_2O_3 reached the maximum of 27.28 mmol/g at the KOH loading of 20%, and then decreased as the loading kept increasing, which was similar to the solid base MgO/ Al_2O_3 and MgO/ZrO₂ reported by D. Jiang et al. [39,40]. The decrease of the total base amount was possibly related to a low average pore and a small surface area [39,40]. When the KOH loading increased from 10% to 20%, the increase of total base amount was possibly due to new phases Al–O–K groups and $\text{K}_2\text{O}\cdot\text{CO}_2$ species formed during the calcination (see Fig. 1). As the KOH loading exceeded 20%, the KOH/ Al_2O_3 had a low average pore and a small surface area (see Table 1), which were due to the blockage of some smaller pore pores. The base sites on the surface were possibly originate from the new phase $\text{K}_2\text{O}\cdot\text{CO}_2$ species and were less with the increase of KOH amount. During the reaction, the

Table 1
Surface areas, average pore size, and pore volume of the studied fresh and spent KOH on alumina.

Catalyst	Surface area (m ² /g)	Average pore size (Å)	Pore volume (cm ³ /g)
γ-Al ₂ O ₃	284.17	6.96	0.53
10% KOH/Al ₂ O ₃	126.8	9.49	0.32
20% KOH/Al ₂ O ₃	58.34	12.87	0.21
30% KOH/Al ₂ O ₃	50.59	7.76	0.11
40% KOH/Al ₂ O ₃	40.28	6.78	0.10
30% KOH/Al ₂ O ₃ -U1	52.45	9.46	0.13
30% KOH/Al ₂ O ₃ -U2	58.64	9.76	0.16
30% KOH/Al ₂ O ₃ -U3	63.89	9.55	0.17
30% KOH/Al ₂ O ₃ -U4	68.35	9.10	0.18
30% KOH/Al ₂ O ₃ -W	245.08	6.26	0.40

Table 2
The surface basicity of the catalyst from CO₂-TPD.

Catalysts	Peak temperature (°C)		Basicity amount (mmol/g)		Ratio basicity of Peak II/Peak I	Total base amount (mmol/g)
	Peak I	Peak II	Peak I	Peak II		
γ-Al ₂ O ₃	139	514	0.98	1.12	1.14	2.10
10% KOH/Al ₂ O ₃	136	553	9.22	14.04	1.52	23.25
20% KOH/Al ₂ O ₃	147	553	10.78	16.50	1.53	27.28
30% KOH/Al ₂ O ₃	135	553	4.80	10.43	2.17	15.23
40% KOH/Al ₂ O ₃	135	553	3.35	8.57	2.56	11.92
30% KOH/Al ₂ O ₃ -U1	171	560	11.33	25.87	2.28	37.20
30% KOH/Al ₂ O ₃ -U2	192	552	10.19	24.23	2.38	34.42
30% KOH/Al ₂ O ₃ -U3	189	550	10.64	18.41	1.73	34.35
30% KOH/Al ₂ O ₃ -U4	182	559	12.45	21.25	1.71	34.11
30% KOH/Al ₂ O ₃ -W	100/255	530	0.50/7.0	8.39	1.20	15.79

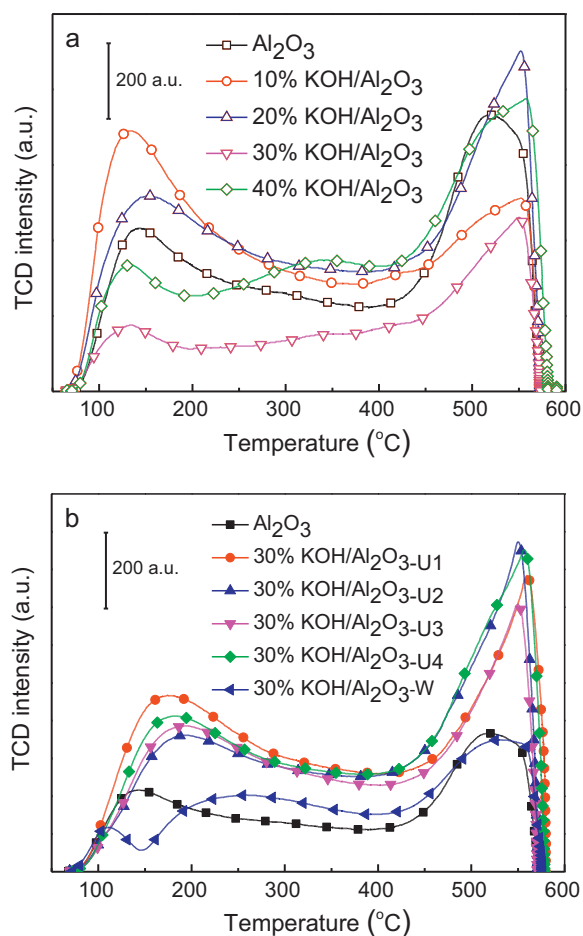


Fig. 3. CO₂-TPD profiles for γ-Al₂O₃, fresh KOH/Al₂O₃, used 30%KOH/Al₂O₃, and water-washing 30%KOH/Al₂O₃.

K₂O·CO₂ species were continually released into reaction medium. After the 30%KOH/Al₂O₃ were reused, the average pore and surface area became larger (see Table 1), and the total base amount were more than fresh 30%KOH/Al₂O₃. Meanwhile, water-washing 30%KOH/Al₂O₃ exhibited more basicity amount than γ-Al₂O₃. It was deduced that Al–O–K groups existed on the surface, which agreed with XRD patterns (Fig. 1). It was found that the basicity ratio of two peaks increased with the increase of KOH loading in Table 2. The ratio had a decline trend after the catalysts reusing for four times. The ratio of the water-washing catalyst was closed to that of γ-Al₂O₃. Table 2 showed that the basicity amount and basicity ratio were responsible for activity during the transesterification.

3.1.5. X-ray fluorescence (XRF)

XRF was used to determine the potassium content before and after the reaction of 30%KOH/Al₂O₃ and water-washing 30%KOH/Al₂O₃. Table 3 showed that about 3% potassium of 30%KOH/Al₂O₃ was leached from the surface each test. Corresponding to BET result of the used catalysts, used 30%KOH/Al₂O₃ had a higher surface area, average pore size, and pore volume than that of fresh 30%KOH/Al₂O₃. This suggested that the part of the species containing potassium on the catalyst surface was leached from the surface. Combining with the results of FT-IR, the leached species were K₂O·CO₂ species. But the potassium could not be wash out completely by water based on the result of water-washing 30%KOH/Al₂O₃, which proved the new phase (Al–O–K) compound was stabilized during polar solvents, like water.

Table 3
Potassium, aluminum and ratio of aluminum/potassium of the catalysts from XRF analysis.

Catalyst	Al(wt%)	K(wt%)	Al/K
Fresh 30% KOH/Al ₂ O ₃	36.65	22.44	1.63
30% KOH/Al ₂ O ₃ -U1	37.42	21.90	1.71
30% KOH/Al ₂ O ₃ -U2	37.60	21.40	1.76
30% KOH/Al ₂ O ₃ -U3	38.57	19.81	1.95
30% KOH/Al ₂ O ₃ -U4	38.92	19.01	2.05
30% KOH/Al ₂ O ₃ -W	51.12	1.27	40.25

Table 4
Effect of KOH loading on γ -Al₂O₃ for transesterification.

Catalyst	Conversion of cis-3-hexen-1-ol (%)	Selectivity of cis-3-hexen-1-yl acetate (%)
γ -Al ₂ O ₃	0.0	0.0
10% KOH/Al ₂ O ₃	8.4	100
20% KOH/Al ₂ O ₃	40.5	100
30% KOH/Al ₂ O ₃	59.3	100
40% KOH/Al ₂ O ₃	59.0	100

Reaction conditions: 0.05 mol cis-3-hexen-1-ol; 0.1 mol ethyl acetate; 5 g catalyst; reaction temperature, 88 °C; reaction time, 120 min; atmospheric pressure.

3.2. Catalytic performance

3.2.1. Effect of KOH loading on Al₂O₃

To investigate the effect of KOH loading on the activity of the KOH/ γ -Al₂O₃ catalysts, several KOH/ γ -Al₂O₃ catalysts with different amounts of KOH were prepared and their catalytic performances were tested. It should be mentioned firstly that two series of reaction data (conversion and selectivity), which were calculated on the basis of cis-3-hexen-ol, were given in Table 4. As listed in Table 4, the selectivity of cis-3-hexen-1-yl acetate was 100% over all catalysts. The cis-3-hexen-1-ol conversion increased from 8.4% to 59.3%, as the KOH amount increased from 10% to 30%. However, there was little improvement in the cis-3-hexen-1-yl acetate after the KOH amount was above 30%. The fresh Al₂O₃ had no catalytic activity on the transesterification. Thus the optimum catalyst was 30%KOH/Al₂O₃.

3.2.2. Effect of reaction parameters over 30% KOH/Al₂O₃

30%KOH/Al₂O₃ was selected for further study because of its excellent performance. The effect of catalyst amount in the range of 4–12% (relative to weight of cis-3-hexen-1-ol) on the conversion of cis-3-hexen-1-ol in the transesterification was investigated and the results were shown in Fig. 4. The results showed that when the amount of catalysts was not sufficient (10%), the reaction could not reach equilibrium for 120 min. However, a further increase in the amount of 30%KOH/Al₂O₃ from 4% to 10% led to a slow increase in cis-3-hexen-1-ol conversion. When the amount of catalysts exceeded 10%, the conversion of cis-3-hexen-1-ol was independent of the amount of 30%KOH/Al₂O₃. Therefore, this indicated that a chemical equilibrium had been reached due to the reversible nature of the reaction. 10% was a suitable catalyst amount in this experimental system.

The effect of reaction temperature on the cis-3-hexen-1-ol conversion was summarized in Fig. 5. The reaction temperature was

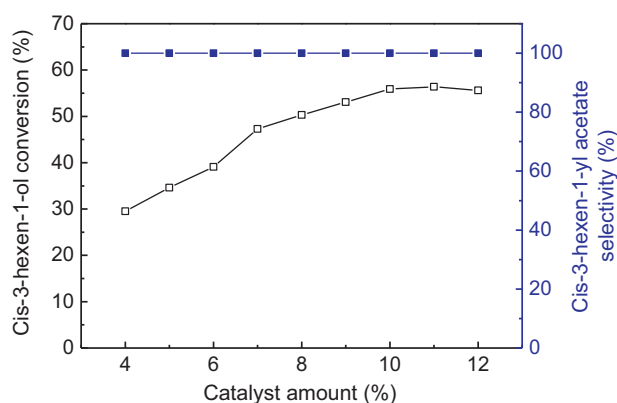


Fig. 4. Effect of catalyst amount on cis-3-hexen-1-ol conversion and cis-3-hexen-1-yl acetate selectivity. Reaction conditions: 0.05 mol cis-3-hexen-1-ol; 0.10 mol ethyl acetate; catalyst, 30%KOH/Al₂O₃; reaction temperature, 88 °C; reaction time, 120 min; atmospheric pressure.

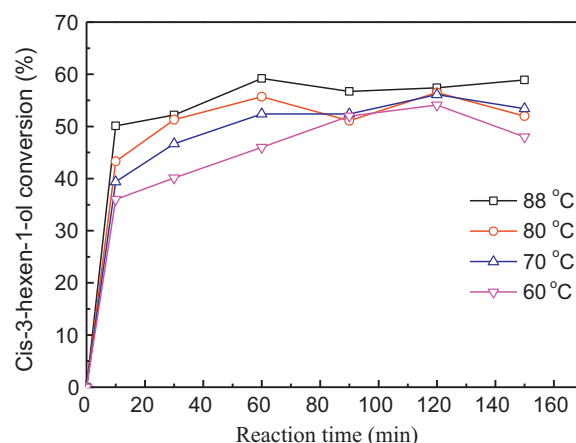


Fig. 5. Effect of reaction time and temperature. Reaction conditions: 0.05 mol cis-3-hexen-1-ol; 0.1 mol ethyl acetate; 0.5 g 30% KOH/Al₂O₃; atmospheric pressure. All of cis-3-hexen-1-yl acetate selectivity was 100%.

varied between 60 °C and 88 °C. As can be seen in Fig. 5, the reaction equilibrium was affected significantly by the reaction temperature. At 60 °C, the reaction reached equilibrium in 120 min, while the time was 60 min at 88 °C. It can be expected that the reaction could proceed more rapidly at a temperature higher than 88 °C. However, the reaction mixture (the molar ratio of cis-3-hexen-1-ol to ethyl acetate was 1:2) cannot be heated to a temperature exceeded 88 °C under atmospheric pressure for the low boiling point of ethyl acetate. The equilibrium conversion of cis-3-hexen-1-ol increased with the reaction temperature. Therefore, the optimizing reaction temperature and time were 88 °C and 120 min. The reaction time was 120 min for guaranteeing the reaction reached equilibrium completely.

The molar ratio of cis-3-hexen-1-ol to ethyl acetate is one of the important factors that affected the conversion of cis-3-hexen-1-ol. Stoichiometrically, one mole of cis-3-hexen-1-ol was required for each mole ethyl acetate. In practice, a higher molar ratio was employed in order to drive the reaction toward completion and produced more cis-3-hexen-1-yl acetate as products. As shown in Fig. 6, when the molar ratio of cis-3-hexen-1-ol to ethyl acetate was increased, the cis-3-hexen-1-ol conversion increased, and the highest conversion (59.3%) was obtained at a cis-3-hexen-1-ol to ethyl acetate molar ratio of 1:2. When further increasing the molar ratio over 1:2, the conversion decreased significantly.

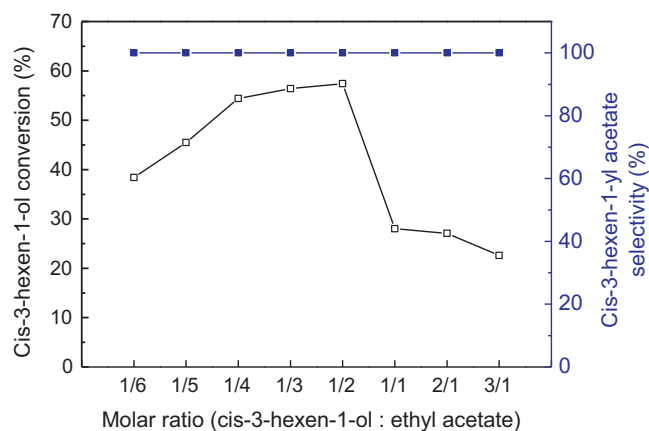


Fig. 6. Effect of the molar ratio of cis-3-hexen-1-ol/ethyl acetate. Reaction conditions: 0.05 mol cis-3-hexen-1-ol; 0.5 g 30%KOH/Al₂O₃; reaction temperature, 88 °C; reaction time, 120 min; atmospheric pressure.

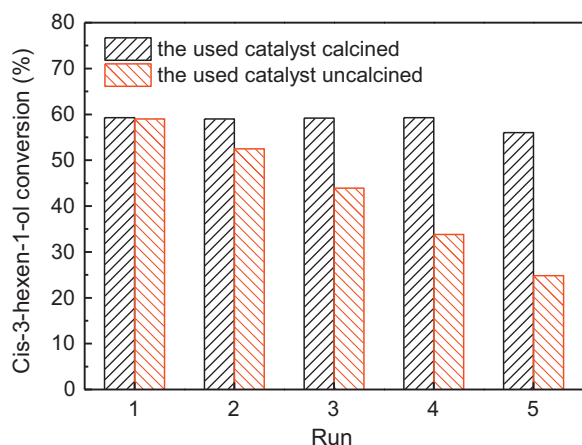


Fig. 7. Reusability of 30% KOH/Al₂O₃ on the transesterification. Reaction conditions: 0.05 mol cis-3-hexen-1-ol; 0.1 mol ethyl acetate; 0.5 g 30% KOH/Al₂O₃; reaction temperature, 88 °C; reaction time, 120 min; atmospheric pressure.

Therefore, the optimum molar ratio of cis-3-hexen-1-ol to ethyl acetate to produce cis-3-hexen-1-yl acetate was approximately 1:2.

3.2.3. Reusability of the catalyst

The reusability of the catalyst is very important for its commercial application. Therefore, the recyclability of 30%KOH/Al₂O₃ was investigated (Fig. 7). After each experiment, the used 30%KOH/Al₂O₃ catalyst was filtered, dried at 120 °C overnight. As can be seen in Fig. 7, the conversion decreased from 59.3% to 24.8% after five cycles. The recyclability of KOH/Al₂O₃ was similar to KF/Al₂O₃ [15] and K₂CO₃/Al₂O₃ [41]. The activity of the used 30%KOH/Al₂O₃ catalyst without calcination decreased due to the leach out of potassium (see Table 3) and the deactivation of K₂O·CO₂ species. While the used 30%KOH/Al₂O₃ catalyst was calcined at 500 °C for 3 h, the activity of 30%KOH/Al₂O₃ catalyst was able to largely maintain its overall catalytic activity for at least five times. When the used 30%KOH/Al₂O₃ catalyst was calcined, the active sites were activated again and the catalyst would have enough number of active sites in successive runs. This feature made the 30%KOH/Al₂O₃ more attractive for potential application in the synthesis of cis-3-hexen-yl acetate in the flavor industry.

3.3. Discussion

According to corroborating data provided by the characterization techniques (XRD, FT-IR, CO₂-TPD, BET, and XRF), a catalyst model and a plausible mechanism for this transesterification were proposed in Fig. 8. The excellent catalytic performance of 30%KOH/Al₂O₃ should be originated from the abundant surface oxygen-containing species. The basicity of oxygen in K₂O·CO₂ species were stronger than that in Al–O–K groups [32] and Al–O–Al groups.

Generally, a new phase of K₂O and Al–O–K were generated through the reaction KOH with γ -Al₂O₃ [21,27,32]. However, they have different opinions on the main active sites. D. M. Alonso and H. B. Ma et al. considered the Al–O–K groups were responsible for the activity of KOH/Al₂O₃ [41,42]. While H. Liu and W. Xie et al. thought K₂O species and Al–O–K groups on the surface were probably the main active sites [21,32]. The Al–O–K groups had lower catalytic activity and basicity than K₂O phase [32]. From Fig. 1, K₂O phase was not observed clearly. These results did not agree well with the result of KI/Al₂O₃ and KNO₃/Al₂O₃ reported by W. Xie et al. [21,22] and KOH/Al₂O₃ [27]. While the bands of CO₃²⁻ were observed clearly from Fig. 2. There was a possible reason for K₂O species reacting with CO₂ forming a specie like K₂CO₃. Because the K₂O species had high activity and adsorbed CO₂ easily in air (K₂O + CO₂ → K₂O·CO₂). During the reaction process, a part of K₂O·CO₂ species was dissolved in the reaction medium and leached away, which agreed with the result of BET and XRF. The fresh 30% KOH/Al₂O₃ was washed, the K₂O·CO₂ species was washed out (Fig. 2), but the Al–O–K groups still existed (Fig. 1). These results agreed with that of XRD (Fig. 1) and FT-IR (Fig. 2). The water-washing 30%KOH/Al₂O₃ had no activity for transesterification. It was deduced that the K₂O·CO₂ species was possibly responsible for the activity of KOH/Al₂O₃.

The catalytic activity increased with the increasing of KOH amount (see Table 4). However, the activity was little improvement after the amount of KOH was above 30%. In addition, the typical diffraction peaks of γ -Al₂O₃ at 2 θ value of 37° and 46° weakened as the amount of KOH was above 20% (see Fig. 1). It was deduced that Al–O–K groups were firstly formed and few K₂O·CO₂ species were generated as the increasing of KOH amount from 10% to 30%. When all Al–O–H groups were transformed into Al–O–K groups, more K₂O·CO₂ species were generated. With the amount of KOH above 30%, the catalyst had smaller surface areas and pore size (Table 1). Therefore, the activity was little improvement after the amount of KOH was above 30%. After the used 30%KOH/Al₂O₃

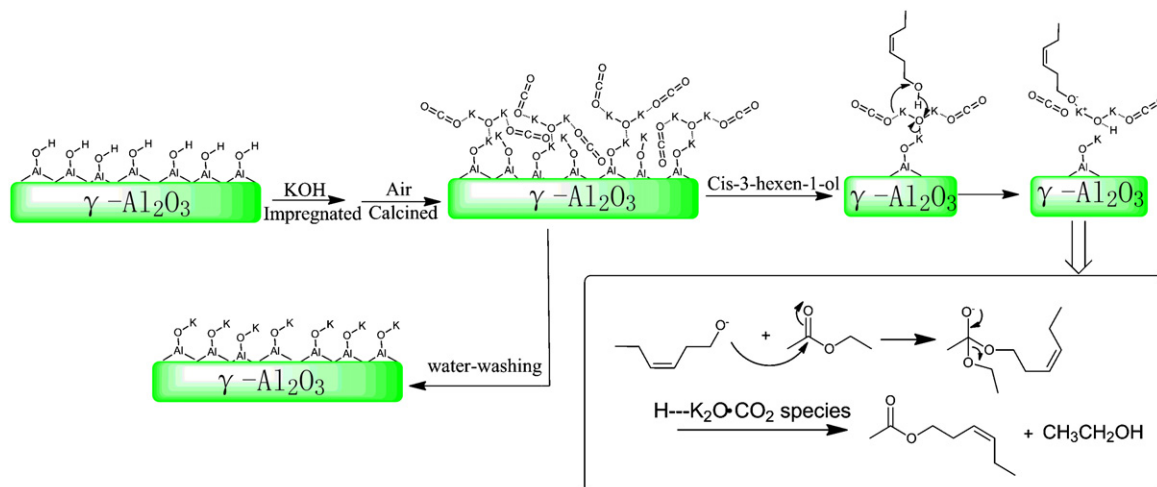


Fig. 8. The catalyst model and a plausible reaction mechanism for transesterification.

was calcined, the $K_2O\text{-CO}_2$ species was formed again. The water-washing 30%KOH/ Al_2O_3 had no activity for transesterification. It was possible that $K_2O\text{-CO}_2$ species were washed out (see Fig. 2) and the Al–O–K groups still existed on the surface of 30%KOH/ Al_2O_3 (see Fig. 1). Therefore, $K_2O\text{-CO}_2$ species might be the major active species on KOH/ Al_2O_3 , and Al–O–K groups was inactive for cis-3-hexen-yl acetate synthesis.

Therefore, the strong base oxygen from $K_2O\text{-CO}_2$ species on the catalyst could make cis-3-hexen-1-ol forming nucleophile ($C_6H_{11}O^-$), and then $K_2O\text{-CO}_2$ species acquired hydrogen cation forming H- $K_2O\text{-CO}_2$ species, which were dissolved in the reaction medium. The nucleophile attacked the carbonyl group of ethyl acetate forming the tetrahedral intermediate; then, the ethoxy departed quickly from the tetrahedral intermediate. The ethoxy gets hydrogen from H- $K_2O\text{-CO}_2$ species, while potassium material stayed in the reaction medium. Many articles have reported that alkali and alkali earth species from catalysts containing alkali and alkali earth dissolved in the reaction medium, and most of the catalysts were formed homogeneous-heterogeneous system [32,43–47]. The $K_2O\text{-CO}_2$ species and Al–O–K groups in KOH/ Al_2O_3 formed a homogeneous-heterogeneous catalytic system. The deactivation of catalysts was for leaching of $K_2O\text{-CO}_2$ species.

4. Conclusions

The heterogeneous catalyst KOH/ Al_2O_3 can be used as solid base catalyst for cis-3-hexen-1-yl acetate via transesterification. The optimum conditions was 30%KOH/ Al_2O_3 , 10% of catalyst, 1:2 cis-3-hexen-1-ol to ethyl acetate molar ratio, reaction time 2 h and temperature 88 °C. At the optimum conditions, the highest conversion of 59.3% was obtained. According to characterization results, KOH on the surface of $\gamma\text{-Al}_2O_3$ transformed into Al–O–K groups and $K_2O\text{-CO}_2$ species through reaction with $\gamma\text{-Al}_2O_3$. Fresh 30%KOH/ Al_2O_3 washed by water without active, $K_2O\text{-CO}_2$ disappeared while Al–O–K groups existed on the surface of the catalyst. Therefore, $K_2O\text{-CO}_2$ species might be the major active species on KOH/ Al_2O_3 , and Al–O–K groups was inactive for cis-3-hexen-yl acetate synthesis. The leaching of $K_2O\text{-CO}_2$ species was the main reason for the deactivation of catalysts.

Acknowledgements

Authors thank the financial support from National Key Technology R&D Program (Grant No. 2012BAD32B08), National Basic Research Program (Grant No. 2011CB710806), National Natural Science Foundation of China (Grant No. 20906051), and the Ph.D. Programs Foundation of Ministry of Education of China (Grant No. 20113221110010).

Appendix A. Supplementary data

Supplementary data associated with this article can be found, in the online version, at <http://dx.doi.org/10.1016/j.apcata.2013.01.015>.

References

- [1] H.D. Belitz, W. Grosch, P. Schieberle, *Food Chemistry*, fourth ed., Springer, 2009.
- [2] S. Horst, P. Johannes, *Common Fragrance and Flavor Materials*, fifth ed., Wiley-VCH, Darmstadt, 2006.
- [3] W.D. Chiang, S.-W. Chang, C.-J. Shieh, *Process Biochem.* 38 (2003) 1193–1199.
- [4] K. Nakane, T. Hotta, T. Ogihara, N. Ogata, S. Yamaguchi, *J. Appl. Polym. Sci.* 106 (2007) 863–867.
- [5] M. Liaquat, *J. Mol. Catal. B: Enzym.* 68 (2011) 59–65.
- [6] S. Bourg-Garros, N. Razafindramboa, A.A. Pavia, *Biotechnol. Bioeng.* 59 (1998) 495–500.
- [7] S. Bourg-Garros, N. Razafindramboa, A.A. Pavia, *Enzyme Microb. Tech.* 22 (1998) 240–245.
- [8] S. Bourg-Garros, N. Razafindramboa, A. Pavia, *J. Am. Oil Chem. Soc.* 74 (1997) 1471–1475.
- [9] S. Velusamy, S. Borpuzari, T. Punniyamurthy, *Tetrahedron* 61 (2005) 2011–2015.
- [10] G. Bartoli, M. Bosco, R. Dalpozzo, E. Marcantoni, M. Massaccesi, L. Sambri, *Eur. J. Org. Chem.* (2003) 4611–4617.
- [11] C.L. Xu, J. Sun, B.B. Zhao, Q.A. Liu, *Appl. Catal. B: Environ.* 99 (2010) 111–117.
- [12] D. Cantrell, L. Gillie, A. Lee, K. Wilson, *Appl. Catal. A: Gen.* 287 (2005) 183–190.
- [13] W. Xie, H. Peng, L. Chen, *Appl. Catal. A: Gen.* 300 (2006) 67–74.
- [14] C. Murugan, H.C. Bajaj, *Fuel Process. Technol.* 92 (2011) 77–82.
- [15] P. Qiu, B. Yang, C. Yi, S. Qi, *Catal. Lett.* 137 (2010) 232–238.
- [16] Y.M. Dong, X.Q. Chen, C.X. Zhao, T.S. Zhao, *J. Mol. Catal. A: Chem.* 331 (2010) 125–129.
- [17] X.Q. Chen, Y.M. Dong, C.X. Zhao, T.S. Zhao, *Energy Fuels* 22 (2008) 3571–3574.
- [18] Y. Feng, N. Yin, Q. Li, J. Wang, M. Kang, X. Wang, *Catal. Lett.* 121 (2008) 97–102.
- [19] H. Kabashima, H. Tsuji, S. Nakata, Y. Tanaka, H. Hattori, *Appl. Catal. A: Gen.* 194–195 (2000) 227–240.
- [20] P. Claus, M. Lucas, B. Luecke, T. Berndt, P. Birke, *Appl. Catal. A: Gen.* 79 (1991) 1–18.
- [21] W. Xie, H. Peng, L. Chen, *Appl. Catal. A: Gen.* 300 (2006) 67–74.
- [22] W. Xie, H. Li, J. Mol. Catal. A: Chem. 255 (2006) 1–9.
- [23] M. Zabeti, W.M.A.W. Daud, M.K. Aroua, *Appl. Catal. A: Gen.* 366 (2009) 154–159.
- [24] N. Boz, N. Degirmenbasi, D.M. Kalyon, *Appl. Catal. B: Environ.* 89 (2009) 590–596.
- [25] C. Xu, J. Sun, B. Zhao, Q. Liu, *Appl. Catal. B: Environ.* 99 (2010) 111–117.
- [26] H. Ma, S. Li, B. Wang, R. Wang, S. Tian, *J. Am. Oil Chem. Soc.* 85 (2008) 263–270.
- [27] K. Noiroj, P. Intarapong, A. Luengnarumitchai, S. Jai-In, *Renew. Energy* 34 (2009) 1145–1150.
- [28] E. Rashtizadeh, F. Farzaneh, M. Ghandi, *Fuel* 89 (2010) 3393–3398.
- [29] S.L.G. Husheer, J.G. Thompson, A. Melnitchenko, *J. Solid State Chem.* 147 (1999) 624–630.
- [30] C. Murugan, H.C. Bajaj, R.V. Jasra, *Catal. Lett.* 137 (2010) 224–231.
- [31] S.U. Rege, R.T. Yang, *Chem. Eng. Sci.* 56 (2001) 3781–3796.
- [32] H. Liu, L. Su, F. Liu, C. Li, U.U. Solomon, *Appl. Catal. B: Environ.* 106 (2011) 550–558.
- [33] B.W. Krupay, Y. Amenomiya, *J. Catal.* 67 (1981) 362–370.
- [34] Y. Amenomiya, G. Pleizier, *J. Catal.* 76 (1982) 345–353.
- [35] Y. Amenomiya, *J. Catal.* 55 (1978) 205–212.
- [36] L. Fernández-Carrasco, E. Vázquez, *Fuel* 88 (2009) 1533–1538.
- [37] P. Sun, D. Yu, K. Fu, M. Gu, Y. Wang, H. Huang, H. Ying, *Catal. Commun.* 10 (2009) 1345–1349.
- [38] Y. Dong, X. Chen, C. Zhao, T. Zhao, *J. Mol. Catal. A: Chem.* 331 (2010) 125–129.
- [39] D. Jiang, G. Pan, B. Zhao, G. Ran, Y. Xie, E. Min, *Appl. Catal. A: Gen.* 201 (2000) 169–176.
- [40] D. Jiang, B. Zhao, Y. Xie, G. Pan, G. Ran, E. Min, *Appl. Catal. A: Gen.* 219 (2001) 69–78.
- [41] D.M. Alonso, R. Mariscal, R. Moreno-Tost, M.D.Z. Poves, M.L. Granados, *Catal. Commun.* 8 (2007) 2074–2080.
- [42] H.B. Ma, S.F. Li, B.Y. Wang, R.H. Wang, S.J. Tian, *J. Am. Oil Chem. Soc.* 85 (2008) 263–270.
- [43] J. Ni, D. Rooney, F.C. Meunier, *Appl. Catal. B: Environ.* 97 (2010) 269–275.
- [44] S.I. Fujita, B.M. Bhanage, D. Aoki, Y. Ochiai, N. Iwasa, M. Arai, *Appl. Catal. A: Gen.* 313 (2006) 151–159.
- [45] M.C.G. Albuquerque, I. Jiménez-Urbistondo, J. Santamaría-González, J.M. Mérida-Robles, R. Moreno-Tost, E. Rodríguez-Castellón, A. Jiménez-López, D.C.S. Azevedo, C.L. Cavalcante Jr., P. Maireles-Torres, *Appl. Catal. A: Gen.* 334 (2008) 35–43.
- [46] J.P. Tessonnier, B. Louis, S. Rigoleto, M.J. Ledoux, C. Pham-Huu, *Appl. Catal. A: Gen.* 336 (2008) 79–88.
- [47] H. Sun, K. Hu, H. Lou, X. Zheng, *Energy Fuels* 22 (2008) 2756–2760.